REMOVAL OF INTERFERENCE LINE NOISE IN JERS-1 SAR IMAGE

Hiroshi Kimura and Takashi Nakamura
Faculty of Engineering, Gifu University
1-1 Yanagido, Gifu-shi, 501-11 Japan

1. Introduction

The synthetic aperture radar (SAR) onboard the Japanese Earth Resources Satellite-1 (JERS-1) has been in operation since April 1992. JERS-1 SAR is one of the promising sensors for remote sensing, operating at L-band (24 cm wavelength), because it can image earth surfaces under all-weather condition and advanced applications such as interferometry and polarimetry draw scientific attention[1][2].

JERS-1 SAR images usually show terrain, but bright line noise often appears in the images of urban and suburban areas. It is known that this noise is not due to the anomaly of the onboard hardware and supposed that it is possibly caused by interference with ground-based radar[3]. This interference noise degrade image quality and disturb use of radar images. In fact, JERS-1 SAR observed the Kobe area on February 6, 1995, but unfortunately the image was disturbed by interference noise. This image is the earliest one after the great earthquake on January 17, 1995, from 44-day repeat cycle orbit, Interference noise leads lots of limitation of radar image applications to survey of the Kobe earthquake.

In this paper we show that this type of noise in JERS-1 SAR images are removable through a certain signal processing. We first give an example of the image interfered with noise and characteristics of the noise. Next, we present model of received signal, noise and image output. Finally, we show a simple method to remove this interference line noise.

2. Features of interference line noise on JERS-1 SAR images

JERS-1 SAR transmits FM chirp pulses toward earth in the normal direction to the track with the pulse repetition frequency of 1500 to 1600 Hz along moving on orbit with the ground speed of 7 km/s. The center frequency of pulse is 1.275 GHz, and the bandwidth is 15 MHz. Polarization is fixed to horizontal for both transmit and receive. An example of interference line noise in JERS-1 SAR image is shown in Fig. 1. This image is part of Kobe city area at 9:41 JST on February 6, 1995. Interference noise is recognized as bright lines in range direction which appear clearly over the sea surface. Fig. 2 presents variation of received pulse spectra over 5.5 seconds including the area shown in Fig. 1. An envelop of transmit pulse wave is constant, therefore spectrum intensity of received signal is expected to be constant in an average over the bandwidth. However, many line features appear in Fig. 2. As described above, possible cause of line spectrum features is ground-based radar.

Received pulses of JERS-1 SAR are digitized onboard and transmitted to ground stations, and then they are processed by ground-based processor, finally radar images are generated. This processing consists of two steps of pulse compression by de-chirping in range and Doppler sharpening in azimuth or track. Through de-chirping, chirped pulses are compressed to narrow pulses in range, but contrary pulses with a fixed frequency spread over range. Through Doppler sharpening, radar echoes from the earth surface are compressed in azimuth, If pulses from ground-based radar are received in some duration as shown in Fig. 2, they are fully or partially compressed in azimuth,
because they are frequency-

Fig. An example of interference noise in JERS-1 SAR image (Kobe city, Feb. 6, 1995, 9;41 JST).

modulated by relative motion as well as normal radar echoes. This is the reason that pulses from ground-based radar appear bright lines in radar images. In addition, it is expected that if interference noise is removed before de-chirping. bright line noise doesn't appear.

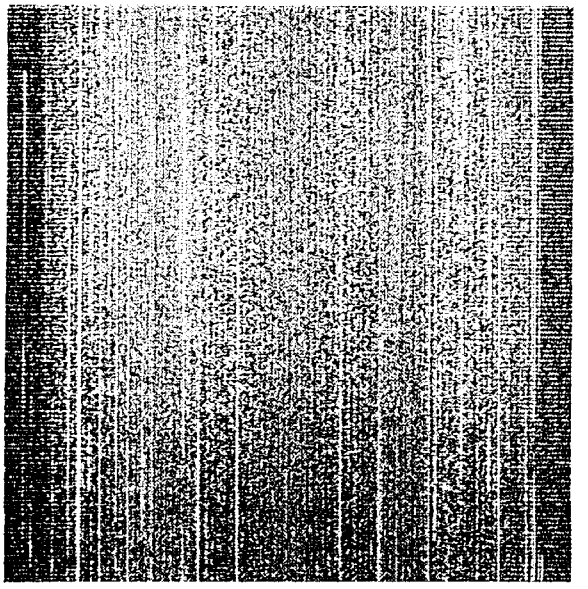

Fig. 2. Spectra of received pulses containing data from the area shown in Fig. 1. Frequency is in horizontal. Time is in vertical. Brightness shows spectrum intensity.

3. Signal and noise model

A simple and convenient method to remove interference noise by ground-based radar is to set a proper threshold to received pulse spectrum. In this section, we describe a model of signal and noise to decide a level of the threshold.

The mean power in a single pulse received from a homogeneous target of normalized cross section, σ^0, can be written

$$P_r = P_s + P_n + P_l = K\sigma^0 + P_n + P_l \qquad (1)$$

where, for convenience,

$$K = \frac{P_t G^2 \lambda^2 G_r}{(4\pi)^3 R^4} A_{ill} .$$

P_s = mean signal power
P_n = mean additive noise power except for interference line noise
P_l = mean interference line noise power
P_t = transmitter power
G = gain of antenna
λ = radar wavelength
G_r = receiver gain
R = slant range
A_{ill} = illuminated area

The mean power in a homogeneous image after compression processing[4] is

$$P_r' = P_s' + P_n' + P_l' = K' n^2 \sigma^0 + nP_n + mP_l \qquad (2)$$

where, for convenience, $K' = \frac{P_t G^2 \lambda^2 G_r}{(4\pi)^3 R^4} a .$

a = resolution cell size on the ground
n = the number of samples integrated through compression processing
m = gain for interference line noise through compression processing

Voltage of received pulse scattered by a homogeneous target can be assumed to be Gaussian with zero-mean[4], Because there is no relation between voltage and frequency over the chirp bandwidth , the power spectrum is exponentially distributed. On the other hand, receive additive noise sources are thermal noise in receiver, quantization noise, thermal radiation from the Earth and propagation noise. We assume here that this noise is white and Gaussian with zero-mean, however it is white on an average, but is Gaussian in short term, such as one receive pulse length 480 μs, Therefore, short time noise power spectrum is exponentially distributed too.

If the threshold P_z is applied to the received signal spectrum with an exponentially probability density, n is given by

$$n = n_0 \int_0^{P_z} \frac{1}{\overline{P}} \exp\left(-\frac{P}{\overline{P}}\right) dP \tag{3}$$

where n_0 is maximum number of samples integrated, $\overline{P}$ is mean power, $K\sigma^0$ or P_n. Here we introduce noise equivalent backscattering coefficient σ_n^0 instead of P_n defined by

$$P_n = K\sigma_n^0 \tag{4}$$

Next, we assume that interference noise power spectrum is exponentially distributed too. Under this assumption, interference noise power is

$$P_I' = A \int_0^{P_z} P \exp(-P/b) dP \tag{5}$$

where A and b are constants to define interference noise distribution, which depends on azimuth location. If A and/or b decreases, P_I' decreases. In case of no interference noise, A and/or b is zero or small enough.

3. Experimental consideration of threshold

We selected two areas on the image shown in Fig. 1. One is urban with high σ^0, and the other is sea surface with small σ^0. Fig. 3 shows relation between processed image power and threshold level for two areas. Image power is normalized by the minimum power of the sea area. Threshold level is normalized by -6.8 dBm which corresponds to P_s from a uniformly distributed target of σ^0= -5.5 dB over illuminated area. In this calculation, JERS-1 SAR parameters are P_t = 325 W, G = 33.5 dB, λ= 0.24 m, G_r= 86 dB, R= 710 km and A_{ill}= 60.5 km^2.

In addition, expected curves of P_s', P_n' and P_I' are drawn in Fig. 3 by fitting model parameters in (2) to (5), i.e. σ^0= -3.7 dB, σ_n^0= -18.2 dB, A= 2.71 mW^{-1} and b= 0.533 W. Considering that measured σ_n^0 of JERS-1 SAR is about -15 to -20 dB [5], it is supposed that noise is dominant in the sea area. Image power of the sea area is supposed to be equal with $P_n'+P_I'$. This is demonstrated well in Fig. 3. Besides, Fig. 3 indicates that the smaller the threshold, the smaller the interference noise is, as expected from (5). In the urban area image, power is expected to be $P_s'+P_n'+P_I'$, and P_s' is supposed to be superior to P_n' and P_I'. This is again demonstrated well in Fig. 3. Moreover, Fig. 3 shows that the power of the urban area decreases as expected from (3), if the threshold decreases to excess. Relation between image power and threshold can be well explained by this signal and noise model.

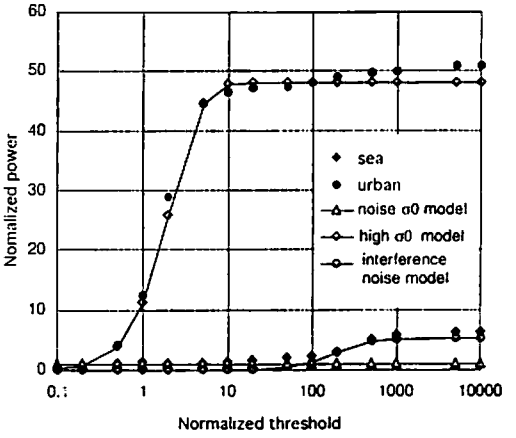

Fig. 3 Experimental and model relation between image power and threshold level.

Here we introduce *SNR* for optimizing the threshold.

$$SNR = P_s' / \left(P_n' + P_I'\right) \tag{6}$$

With the exponential distribution model, *SNR* can be written.

$$SNR = \frac{K'\sigma^0 n_0 \left\{ \int_0^{P_z} \frac{1}{K\sigma^0} \exp\left(-\frac{P}{K\sigma^0}\right) dP \right\}^2}{K\sigma_n^0 \int_0^{P_z} \frac{1}{K\sigma_n^0} \exp\left(-\frac{P}{K\sigma_n^0}\right) dP + A \int_0^{P_z} P \exp\left(-\frac{P}{b}\right) dP} \tag{7}$$

From Fig. 3, *SNR* in the urban area image becomes high with the normalized threshold 10 to 100. However we can expect optimizing the threshold, it may change with σ^0 of a target and probability of

interference noise, i.e. A and b in (5). In scientific use of SAR images, distributed targets are generally more important than hard targets. Therefore, we concentrate on only distributed targets here. Upper boundary of the distributed target σ^0 at L-band and incidence angle of JERS-1 SAR, i.e. 38°, is estimated at -3 dB from [6]. Fig. 4 is *SNR* estimate for two targets, σ^0 = -3 dB and -13 dB as a function of threshold level. The above signal noise model is applied, assuming three cases of interference noise probability. One is the same noise condition as Fig. 1 (Noise 1). Compared to Noise 1, P_I is 10 times in Noise 2 and is one tenth in Noise 3.

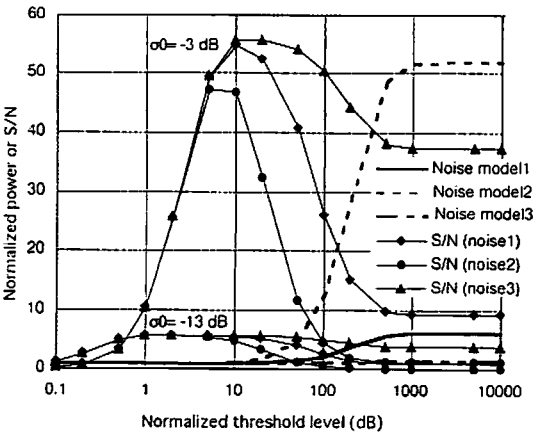

Fig. 4 relation between *SNR* and threshold level.

Fig. 4 indicates that the threshold level 10 (equivalent σ^0=4.5 dB) leads highest *SNR* for both high and moderate σ^0 targets under same or less noise condition compared to Fig. 1. However, under more severe noise condition, the threshold level 5 (equivalent σ^0=1.5 dB) to 10 leads good *SNR* for both σ^0targets. In addition, it is expected that the threshold level 10 don't disturb image power so much, in case of no interference noise. Fig. 5 shows the result of noise removal by applying 10 level threshold. Compared to Fig. 1, interference line noise is suppressed well over the image without depending on target σ^0.

4. Conclusion

We have derived a signal and noise model to express relation between image power and threshold level. An experiment demonstrate that this model explain actual variation of image power. Consideration based on this model leads a choice of threshold. Strict optimum threshold changes with target σ^0 and interference noise probability. However, to remove the interference noise of power being less than 10 dB to the data used here (Fig. 1), optimum threshold equivalent σ^0 is 4.5 dB for general distributed targets. Propriety of this level is also visually confirmed by the image processed by applying this.

Fig. 5 Noise-removed image by equivalent threshold σ^0 = 4.5 dB.

Acknowledgment

JERS-1 SAR data used here is provided by Earth Environment Observation Committee.

References

[1] H.A.Zebker, P.A. Rosen, R.M. Goldstein, A. Gabriel and C.L. Werner, On the derivation of coseismic displacement fields using differential radar interferometry: The Landers earthquake, J. Geophys. Res., 99, 19,617-19,634, 1994.

[2] D. Massonnet, P. Briole and A. Arnaud, Deflation of Mount Etna monitored by spaceborne radar interferometry, Nature, 375, 567-570,1995.

[3] Y. Nemoto, Status of JERS-1 SAR, JERS-1 Information exchange meeting, 29-37, 1993.

[4] F.T. Ulaby, R.K. Moore and A.K. Fung, Microwave remote sensing vol. II, Artech House, 476-483,1982.

[5] B. Chapman, M. Alves and A. Freeman, Validation and calibration of J-ERS-1 SAR imagery, Final Report of JERS-1/ERS-1 System Verification Program vol. I, MITI and NASDA, 75-91,1995.

[6] A. Freeman, C, Kramer, M. Alves and B. Chapman, Amazon rain forest classification using J-ERS-1 SAR data, Final Report of JERS-1/ERS-1 System Verfication Program vol. II, MITI and NASDA, 343-353, 1995.